The Journal of Immunology

Inhibition of the Deubiquitinase Usp14 Diminishes Direct MHC Class I Antigen Presentation

Amy L. Palmer, Annemieke de Jong, Yves Leestemaker, Paul P. Geurink, Ruud H. Wijdeven, Huib Ovaa and Brian P. Dolan

J Immunol published online 27 December 2017
http://www.jimmunol.org/content/early/2017/12/27/jimmunol.1700273

The Journal of Immunology is published twice each month by
The American Association of Immunologists, Inc.,
1451 Rockville Pike, Suite 650, Rockville, MD 20852

Print ISSN: 0022-1767 Online ISSN: 1550-6606.

Published December 27, 2017, doi:10.4049/jimmunol.1700273

Inhibition of the Deubiquitinase Usp14 Diminishes Direct MHC Class I Antigen Presentation

Amy L. Palmer,* Annemieke de Jong,† Yves Leestemaker,†,‡ Paul P. Geurink,†,‡ Ruud H. Wijdeven,†,‡ Huib Ovaa,†,‡ and Brian P. Dolan*

Infected or transformed cells must present peptides derived from endogenous proteins on MHC class I molecules to be recognized and targeted for elimination by Ag-specific cytotoxic T cells. In the first step of peptide generation, proteins are degraded by the proteasome. In this study, we investigated the role of the ubiquitin-specific protease 14 (Usp14), a proteasome-associated deubiquitinase, in direct Ag presentation using a ligand-stabilized model protein expressed as a self-antigen. Chemical inhibition of Usp14 diminished direct presentation of the model antigenic peptide, and the effect was especially pronounced when presentation was restricted to the defective ribosomal product (DRiP) form of the protein. Additionally, presentation specifically from DRiP Ags was diminished by expression of a catalytically inactive form of Usp14. Usp14 inhibition did not appreciably alter protein synthesis and only partially delayed protein degradation as measured by a slight increase in the half-life of the model protein when its degradation was induced. Taken together, these data indicate that functional Usp14 enhances direct Ag presentation, preferentially of DRiP-derived peptides, suggesting that the processing of DRiPs is in some ways different from other forms of Ag. ***The Journal of Immunology*****, 2018, 200: 000–000.**

Activated cytotoxic $CD8^+$ T lymphocytes are able to recognize short antigenic peptides bound to MHC class I molecules expressed at the surface of infected or transformed cells. These peptides are generated as proteins synthesized within the target cell are degraded, and the peptides are subsequently transported into the endoplasmic reticulum where they bind to MHC class I molecules. The peptide–MHC complex then traffics to the cell surface where it can be surveyed by $CD8^+$ T cells. The process of peptide generation, transport, loading, and migration of complexes to the cell surface is known as direct Ag presentation.

Protein degradation is the critical first step in Ag processing. Generation of antigenic peptides is the result of proteasome-mediated degradation of the precursor protein, although there are notable exceptions to this rule (1). Proteins are usually targeted to the proteasome through the addition of ubiquitin moieties to the substrate. Before the protein can efficiently be degraded by the proteolytic activities present in the 20S barrel of the proteasome, the ubiquitin chains are further processed and removed by deubiquitinating enzymes (DUBs). One DUB, Rpn11, is an integral part of the 19S lid, whereas two other DUBs, Uch37 and ubiquitin-specific protease 14 (Usp14), reversibly interact with the 19S lid (2, 3). Covalent modification of antigenic substrates with ubiquitin molecules often enhances presentation of peptides derived from the ubiquitin-tagged protein (4, 5), and it is therefore likely that deubiquitination of the antigenic substrate by proteasomal-associated DUBs is a necessary step for Ag presentation.

Peptides for direct Ag presentation can be derived from two potential forms of a given protein: retirees and defective ribosomal products (DRiPs) (6, 7). Retired proteins are degraded based on the observed metabolic half-life specific to the protein, whereas DRiPs are rapidly degraded immediately after the protein is synthesized by the ribosome (8, 9). Although both forms of a protein can give rise to peptides that are presented at the cell surface, advanced mass spectrometry experiments have demonstrated that the bulk of peptides at the cell surface are derived from DRiPs (10, 11). How DRiPs gain preferential access to the Ag presentation machinery of a cell is unknown.

In this study, we investigated the role of Usp14 in direct Ag presentation. Using a cell line expressing a model Ag, we demonstrate that inhibition of Usp14 with small molecules negatively impacts direct Ag presentation, and inhibition of Usp14 disproportionally impacts presentation of peptides derived from DRiPs. Expression of dominant-negative (DN) forms of Usp14 also inhibited DRiP presentation. These data support the hypothesis that DRiPs are a distinct subset of substrates necessary for Ag presentation and the activity of Usp14 is required for their presentation.

Materials and Methods

Abs and reagents

The anti–K^b-SIINFEKL mAb 25D-1.16 (12) was a gift of Dr. J. Bennink and Dr. J. Yewdell (National Institute of Allergy and Infectious Diseases) and was coupled to the fluorescent dye Alexa Fluor 647 using protein labeling kits from Molecular Probes (Life Technologies) following the manufacturer's protocol. Rabbit anti-cytoskeletal actin and rabbit anti-Usp14

*Department of Biomedical Sciences, College of Veterinary Medicine, Oregon State University, Corvallis, OR 97331; †Division of Cell Biology II, Netherlands Cancer Institute, 1066 CX Amsterdam, the Netherlands; and ‡Department of Chemical Immunology, Leiden University Medical Center, 2333 ZC Leiden, the Netherlands

ORCID: 0000-0002-0068-054X (H.O.).

Received for publication February 21, 2017. Accepted for publication November 22, 2017.

This work was supported by National Institutes of Health Grants R56AI112588 and R01AI130059 (to B.P.D.).

Address correspondence and reprint requests to Dr. Brian P. Dolan, Oregon State University, 105 Magruder Hall, Corvallis, OR 97331. E-mail address: Brian.Dolan@oregonstate.edu

Abbreviations used in this article: 1B10, 1-(1-(3-chloro-4-fluorophenyl)-2,5-dimethyl-1*H*-pyrrol-3-yl)-2-(piperidin-1-yl)ethan-1-one; BFA, brefeldin A; 1D18, *N*-(2-(1-(4-fluorophenyl)-2,5-dimethyl-1*H*-pyrrol-3-yl)-2-oxoethyl)-*N*-methyl-2,3-dihydrobenzo[*b*][1,4]dioxine-6-sulfonamide; DN, dominant-negative; DRiP, defective ribosomal product; DUB, deubiquitinating enzyme; IU1, 1-[1-(4-fluorophenyl)-2,5-dimethyl-1*H*-pyrrol-3-yl]-2-(1-pyrrolidinyl)ethanone; MFI, mean fluorescence intensity; Rho-Ub-PA, rhodamine-ubiquitin-propargylamide; SCRAP, shield-controlled recombinant antigenic protein; TBS-T, TBS with 0.1% Tween 20; UPR, unfolded protein response; Usp14, ubiquitin-specific protease 14; WT, wild-type.

Abs were from Bethyl Laboratories, whereas goat mAb anti-GFP was from Novus Biologicals. Mouse mAb FK2 for polyubiquitin was from Enzo Life Sciences. IRDye 680LT goat anti-mouse, IRDye 800CW goat anti-rabbit, and IRDye 680LT donkey anti-goat secondary Abs were from LI-COR Biosciences. MG-132 and emetine were from Calbiochem, and brefeldin A (BFA) was from Millipore. 1-[1-(4-Fluorophenyl)-2,5-dimethyl-1*H*-pyrrol-3-yl]-2-(1-pyrrolidinyl)ethanone (IU1) was from Cayman Chemical. Compounds *N*-(2-(1-(4-fluorophenyl)-2,5-dimethyl-1*H*-pyrrol-3-yl)-2-oxoethyl)-*N*-methyl-2,3-dihydrobenzo[*b*][1,4]dioxine-6-sulfonamide (1D18) and 1-(1-(3-chloro-4-fluorophenyl)-2,5-dimethyl-1*H*-pyrrol-3-yl)-2-(piperidin-1-yl)ethan-1-one (1B10) were from Enamine. A Gentest precoated parallel artificial membrane permeability assays plate system was obtained through Corning. BSA was from Amresco and Shield-1 was obtained through Clontech.

Plasmids

The shield-controlled recombinant antigenic protein (SCRAP)–mCherry construct was created using overlapping PCR reactions. The FKB12-destabilization domain containing the SIINFEKL sequence was PCR amplified from the original SCRAP plasmid (13) with primer 1 (5′-TCTAGAGAGCTCCCACCATGGGAGTGCAGGTGGAAACCA-3′) and primer 2 (5′-CTTTTCGAAGTTGATGATCGATTCCGGTTTTA-3′), whereas the SIINFEKL-mCherry portion of the fusion protein was PCR amplified from the plasmid pSC11-mCherry-Ub-SIINFEKL (14) using primer 3 (5′-TCGATCATCAACTTCGAAAAGCTAGTGAGCAAGGGC-GAGGAGGATAAC-3′) and primer 4 (5′-AGATCTCTCGAGCTACTTG-TACAGCTCGTCCATGCCGCCGGTGGA-3′). Individual PCR reactions were purified using a Qiagen PCR purification kit, and 1 μl of each reaction was used as a template for the final PCR reaction where primers 1 and 4 were used to amplify the entire cassette. The final PCR product was digested with SacI and XhoI restriction enzymes and cloned into the pCAGGS expression vector (15). GFP-Usp14 wild-type (WT) and DN constructs were PCR amplified from previously published peGFP-C1 plasmids (16) using the primers 5′-TCATCGAGAGCTCCCACCATG-3′ and 5′-TCGATGAGCTAGCCTATTACT-3′ to introduce SacI and NheI restriction sites. This PCR product was digested with both enzymes and ligated with pCAGGS plasmid. Plasmid DNA was purified using a HiSpeed Midi kit (Qiagen) and used for stable cell line generation.

Cell culture and stable cell line generation

EL4 cells were cultured as previously described (17). Plasmids were digested with ScaI to linearize the vector, purified by ethanol precipitation, and resuspended in sterile water. Approximately 6 μg of linearized DNA was used to transfect 8×10^5 EL4 cells using the Amaxa 96-well shuttle electroporation system (Lonza). Cells were resuspended in transfection solution SF and electroporated using program DS-113. Following transfection, cells were cultured for 1 wk before an initial round of fluorescent sorting at the Oregon State University Flow Cytometry Core Facility using a Beckman Coulter MoFlo XDP cell sorter. Fluorescent protein-positive cells were returned to culture and resorted within 2 wk. The process was repeated until cells were >90% positive for fluorescent protein expression.

Chemical permeability assay

Parallel artificial membrane permeability assays were used to determine the capability of the USP14 inhibitors to passively diffuse across a cellular membrane. Following the manufacturer's protocol with slight modifications, the plate was allowed to warm up to room temperature for at least 30 min. Stock solutions were diluted in PBS. A standard curve was made from 15.6 (limit of detection), 31.25, 62.5, 125, and 250 μM for each compound. Replicates of three wells were used for each compound, including a PBS negative control. The donor plate contained 250 μM in 300 μl of PBS per well of each compound. Then 200 μl of PBS was added to each well in the acceptor plate and placed carefully into the donor plate and incubated at room temperature for 6 h in the dark to prevent chemical deterioration. After incubation was complete the acceptor plate was removed from the donor plate and the concentration of inhibitors was determined from absorbance at 310 nm with UV/visible spectroscopy and calculating permeability using the formula derived by the manufacturer.

Activity-based competition assay using a ubiquitin-based DUB probe

EL4 cells were lysed by sonication (five cycles of 30 s sonication/30 s no sonication) in lysis buffer (50 mM Tris, 250 mM sucrose, 5 mM $MgCl_2$, 1 mM DTT) at 4°C, followed by spinning (16,000 × *g*, 10 min, 4°C). Cell lysates (1 mg/ml) were incubated with indicated concentrations of inhibitor in DMSO (60 min at 37°C) followed by incubation with 0.5 μM rhodamine-ubiquitin-propargylamide (Rho-Ub-PA) (18) for 60 min at 37°C. Labeling reactions were terminated by addition of reducing sample buffer and heating (95°C, 10 min). Proteins were resolved by SDS-PAGE, followed by in-gel fluorescence scanning with a GE Healthcare Life Sciences Typhoon FLA 9500 imager and analyzed with ImageQuant software (excitation/emission wavelength of 496 nm/520 nm).

Ag presentation and flow cytometry

To study presentation of antigenic peptides, cells were chilled on ice for 10 min and resuspended in ice-cold citric acid buffer (0.13 M citric acid and 0.056 M dibasic sodium phosphate [pH 3]) at 1×10^7 cells/ml for 2 min. Ice-cold RPMI 1640 supplemented with HEPES buffer was added to neutralize the acid and cells were washed in PBS and resuspended in warm, complete RPMI 1640 media at 1×10^6 cells/ml. Cells were cultured and at indicated time points in the presence, absence, or removal of 1 μM Shield-1 and processed for flow cytometry analysis. Usp14 chemical inhibitors IU1, 1D18, and 1B10 were used at indicated concentrations. MG-132, a proteasome inhibitor, BFA, an inhibitor of the secretory pathway, and emetine, a protein synthesis inhibitor, were also used in some experiments at 10 μM and added to cells after acid washing had occurred to prevent Ag presentation. At indicated times, aliquots of treated cells (generally 10^5) were removed and stained with Alexa Fluor 647–labeled 25D-1.16 mAb and analyzed by flow cytometry. Briefly, cells were harvested and washed in HBSS (Life Technologies) supplemented with 0.1% BSA. K^b-SIINFEKL expression was measured by staining cells with Alexa Fluor 647–coupled 25D-1.16 mAb for 30 min at 4°C, washing cells and resuspending cells in HBSS/BSA. Cells were analyzed by flow cytometry using an Accuri C6 flow cytometer (BD Biosciences) except for experiments measuring SCRAP-mCherry degradation after Shield-1 removal, in which case a BD CytoFLEX flow cytometer (BD Biosciences) equipped with a yellow laser was used to measure mCherry fluorescence. Flow cytometry data were analyzed using the Accuri C6 software.

Calculations for Ag presentation

Because the SCRAP-mCherry transgene is constitutively expressed as a stable gene in the EL4 cell line, all Ag presentation experiments reported in the present study relied on acid washing cells prior to the start of an experiment to remove existing K^b-SIINFEKL complexes. Cells were analyzed immediately after acid wash as described above by staining with the 25D-1.16 mAb as described above and the mean fluorescence intensity (MFI) levels of both mCherry and K^b-SIINFEKL at this time point were treated as background levels and subtracted from the MFI levels at later indicated time points. SIINFEKL peptides can be derived from different sources in this system, including nascent proteins sensitive to Shield-1 (referred to as non-DRiP substrates), nascent proteins insensitive to Shield-1 treatment (referred to as DRiPs), and previously synthesized protein, stabilized by Shield-1 treatment and subsequently "retired" by removing Shield-1 and inducing degradation (referred to as retirees). The relative contribution of each source of peptide can be calculated. To determine Ag presentation of non-DRiP substrates, the MFI of the population of cells treated with Shield-1 was subtracted from the MFI of the cell population treated with ethanol alone. To determine Ag presentation from DRiP substrates, the MFI of the BFA-treated cells (representing the background levels of Ab staining) was subtracted from the MFI of Shield-1–treated cells. To determine peptide presentation from retirees following Shield-1 removal, the MFI of the population previously treated with ethanol (and therefore lacking a pool of stable substrate to be degraded) was subtracted from the MFI of the population previously treated with Shield-1. To determine the percentage inhibition of presentation we used the following formula: $100 - \{100 \times [(\text{MFI Usp14 inhibitor} - \text{MFI BFA treatment})/(\text{MFI DMSO treatment} - \text{MFI BFA treatment})]\}$, where MFI is the MFI for K^b-SIINFEKL staining for the indicated treatment (treated with Usp14 inhibitor, DMSO, or BFA treatment) and the denominator of the equation defines the range of Ag presentation. When measuring percentage inhibition for DRiP substrates, the recorded MFI measurements were used. When measuring non-DRiP presentation, the MFI of cells treated with Shield-1 was subtracted from the MFI of cells treated with ethanol prior to calculating percentage inhibition. For Ag presentation experiments utilizing EL4/SCRAP-mCherry cells lines stably expressing either WT or DN Usp14, the MFI of K^b-SIINFEKL staining was normalized to the MFI of the mCherry signal to account for differences in SCRAP-mCherry protein in the two cell lines.

Western blots

For Western blot analysis, cells were treated and collected at the indicated times. Cells (10^6) were collected and lysed by boiling in 100 μl of 4× Bolt

LDS sample buffer (Thermo Fisher) containing 10 nM protease inhibitor *N*-ethylmaleimide and Pierce EDTA-free protease inhibitor for 20 min with periodic vortexing. After complete lysis, 100 μl of water containing 1.0 μM DTT was added to each sample and boiled for an additional 10 min. Samples were resolved on 4–12% Bolt Bis-Tris polyacrylamide gels (Thermo Fisher) followed by blotting onto nitrocellulose membranes using the iBlot system and reagents according to the manufacturer's recommendations. Membranes were blocked for 1 h with 5% milk solution in TBS with 0.1% Tween 20 (TBS-T). After blocking, the membranes were incubated with primary Abs in 0.5% milk solution in TBS-T overnight. Membranes were washed with TBS-T for 10 min and incubated with secondary Abs also in 0.5% milk TBS-T for 45 min. The membranes were washed twice with TBS-T and then once with water, and analyzed using an Odyssey infrared imager (LI-COR Biosciences) and LI-COR Biosciences software.

Statistical analysis

Student *t* test analysis, SE, one-way ANOVA, linear regression, and one-phase decay were analyzed using GraphPad Prism software. All experiments were repeated a minimum of three times and representative results are depicted. Unless otherwise noted, SEs on each graph depicted were determined from within-experiment variation.

Results

The small molecule known as IU1 is a known Usp14 inhibitor (19). Two other compounds with structural similarity to IU1 (Fig. 1A), which we term 1D18 and 1B10, were tested for their ability to inhibit Usp14 in an in vitro competition assay. EL4 cell lysates were incubated with the small-molecule inhibitors and then mixed with a fluorescent ubiquitin-based probe, Rho-Ub-PA, which binds to the active site of DUBs in cell lysates and can be visualized by fluorescent scanning after resolving the proteins by SDS-PAGE (16, 18). Inhibitors of DUBs compete with the probe for binding to the DUB, and loss of fluorescence signal indicates that a particular inhibitor targets a specific DUB or DUBs. All three molecules were able to inhibit the activity of a DUB ∼60 kDa in size (Fig. 1B), which corresponds to the size of Usp14 as determined by Western blot (Fig. 1C). Note the slight difference in apparent molecular mass of the band in Fig. 1B and 1C is due to the binding of the fluorescent probe, increasing the apparent size of Usp14 in Fig. 1B relative to Fig. 1C. Both 1B10 and 1D18 inhibited probe binding to Usp14 at concentrations similar to previously reported Usp14 inhibitors in similar assays (16), and statistically significant decreases in probe binding to Usp14 were noted at the highest concentration tested (Fig. 1D, $p < 0.05$). Although IU1 did decrease the level of fluorescent probe interacting with Usp14, the decrease was not statistically significant. We also tested the three small-molecule inhibitors in a membrane permeability assay (Fig. 1E). Both 1B10 and 1D18 traversed an artificial membrane to a greater extant than did IU1.

To test direct presentation of self-antigens from DRiP and non-DRiP sources of peptides, we generated a modified form of a model protein known as SCRAP (13) and replaced the original GFP with mCherry. The complete construct contained the FKBP12 destabilization domain (20), followed by the peptide SIINFEKL and mCherry fluorescent protein. EL4 cells were stably transfected with the SCRAP-mCherry construct and tested for both mCherry expression (Fig. 2A) and K^b-SIINFEKL expression (Fig. 2B).

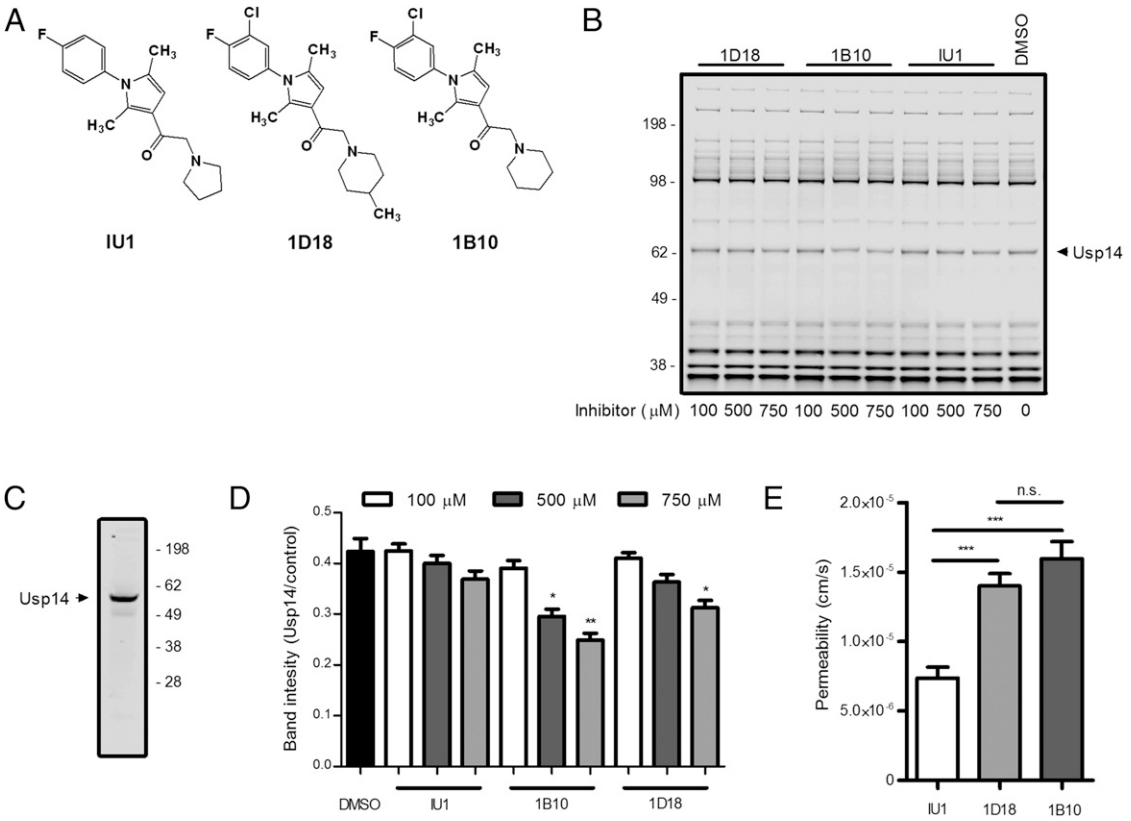

FIGURE 1. Compounds 1D18 and 1B10 are comparable to IU1. Compounds 1D18 and 1B10 were directly assessed against the selective Usp14 inhibitor IU1. (**A**) Schematic depiction of the chemical structures of all three compounds. (**B**) EL4 cell lysates were incubated with each compound of interest at various concentrations indicated for 60 min. Lysates were probed with Rho-Ub-PA and then resolved by SDS-PAGE to assess levels of deubiquitinating activity found throughout the cell. Usp14 is indicated in the figure based on previous experiments (16) and Western blot of Usp14 (**C**). (**D**) Analysis of DUB activity was determined by comparing Usp14 band intensity to the band intensity of a control band. (**E**) Permeability (centimeters per second) was determined by passive diffusion of chemical compounds from one well to another through an artificial membrane after 6 h incubation at room temperature in the dark. $*p < 0.01$, $**p < 0.001$, $***p < 0.0001$. n.s., not significant.

Fluorescent protein in EL4/SCRAP-mCherry cells increased following Shield-1 treatment (Fig. 2A) compared with the parental cell line and did so in a dose-dependent manner (Fig. 2C). Treatment with equivalent amounts of ethanol (the carrier for Shield-1) did not alter the cells in any appreciably manner. A 1.0 μM dose of Shield-1 is sufficient to saturate the cells, similar to other constructs (21). To measure Ag presentation, EL4/SCRAP-mCherry cells were washed in a mild citric acid buffer to remove existing K^b-SIINFEKL from the cell surface and cells were stained with the 25D-1.1.6 mAb at different times. Cells were treated with different compounds to inhibit Ag presentation, such as BFA, MG-132, and emetine, and compared with cells treated with Shield-1 or with ethanol alone. When SCRAP-mCherry degradation was prevented by treatment with Shield-1, there was a decrease in K^b-SIINFEKL levels compared with ethanol-treated cells, although ongoing Ag presentation was still observed and levels of peptide–MHC were higher than in cells treated with inhibitors that completely block Ag presentation (Fig. 2D, 2E). This presentation can be observed in either kinetic (Fig. 2D) or static experiments examining a single time point (Fig. 2E). Because ongoing Ag presentation was detected at a saturating dose of Shield-1 treatment, we conclude that some portion of newly synthesized SCRAP-mCherry is inherently defective, degraded, and yields peptides for Ag presentation, and is thus likely a DRiP. This is consistent with data generated with similar constructs (13, 21, 22).

To determine what impact Usp14 inhibition would have on direct Ag presentation, we incubated acid-washed EL4/SCRAP-mCherry cells with varying concentrations of each inhibitor in the presence or absence of Shield-1 and measured K^b-SIINFEKL after 5 h of treatment. As shown in Fig. 3A, treatment with Usp14 inhibitors diminished, but did not abolish, Ag presentation of peptides from DRiP substrates (i.e., 25D-1.16 staining in the presence of Shield-1 relative to BFA controls). Presentation of peptides from non-DRiP substrates was determined by subtracting the MFI of Shield-1–treated cells from the MFI of ethanol-treated cells (Fig. 3A). Whereas compounds 1D18 and 1B10 slightly diminished presentation of peptides from non-DRiP substrates at the higher concentrations of inhibitor, inhibition of Usp14 by IU1 treatment had no impact on non-DRiP presentation. We also determined the percentage of presentation inhibition for each class of substrate (Fig. 3B) and found that DRiP presentation was more sensitive to Usp14 inhibition than presentation of peptides from non-DRiP substrates.

We next determined the impact of Usp14 on SCRAP-mCherry protein degradation and presentation of peptides from these retired substrates. Cells were treated overnight with Shield-1 to build up a pool of SCRAP-mCherry and then acid washed to remove existing peptide–MHC complexes and cultured in the absence of Shield-1 with or without Usp14 inhibitors. There is a short lag time following Shield-1 removal before mCherry fluorescence rapidly decreases in cells (Fig. 4A). We calculated the half-life of

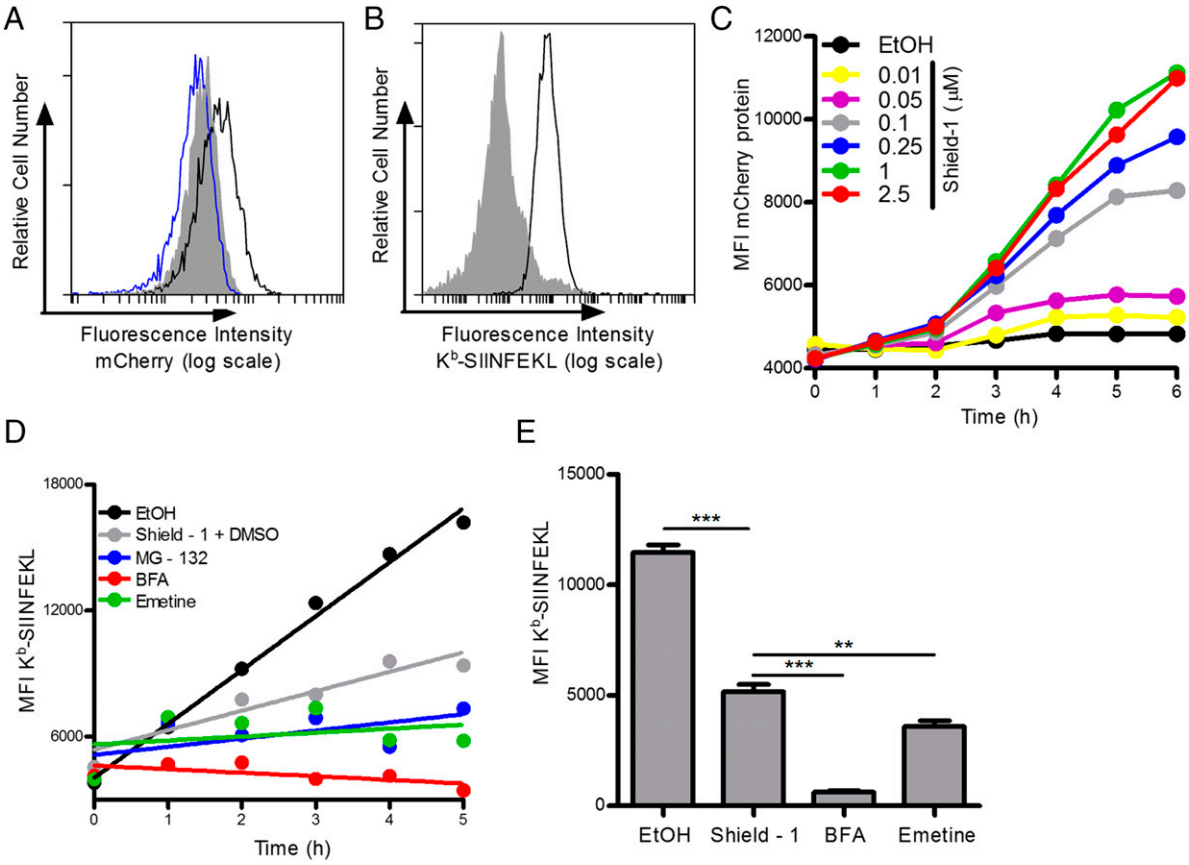

FIGURE 2. Shield-1 prevents the degradation of SCRAP-mCherry in EL4 cells. (**A**) Fluorescent mCherry protein accumulation after 18 h treatment of EL4/SCRAP-mCherry cells with either ethanol (blue trace) or Shield-1 (black trace) compared with parental EL4 cells (shaded). (**B**) K^b-SIINFEKL expressed in SCRAP-mCherry cells first washed in mild acidic buffer (shaded histogram) then treated with ethanol for 5 h (black trace). (**C**) Kinetic accumulation of mCherry protein during 6 h with the addition of various concentrations of Shield-1. (**D**) SCRAP-mCherry cells were treated with vehicle, Shield-1 (1.0 μM), MG-132 (10 μM), BFA (10 μM), or emetine (10 μM) and aliquots of cell suspensions were collected every hour for 5 h. Cells were stained as in (B). A linear regression line of best fit is shown. (**E**) Similar to (D) above, except only one time point (5 h) was measured in triplicate after cells were acid washed and treated with ethanol, Shield-1, BFA, or emetine. Analysis was performed by flow cytometry. $^{**}p < 0.01$, $^{***}p < 0.001$.

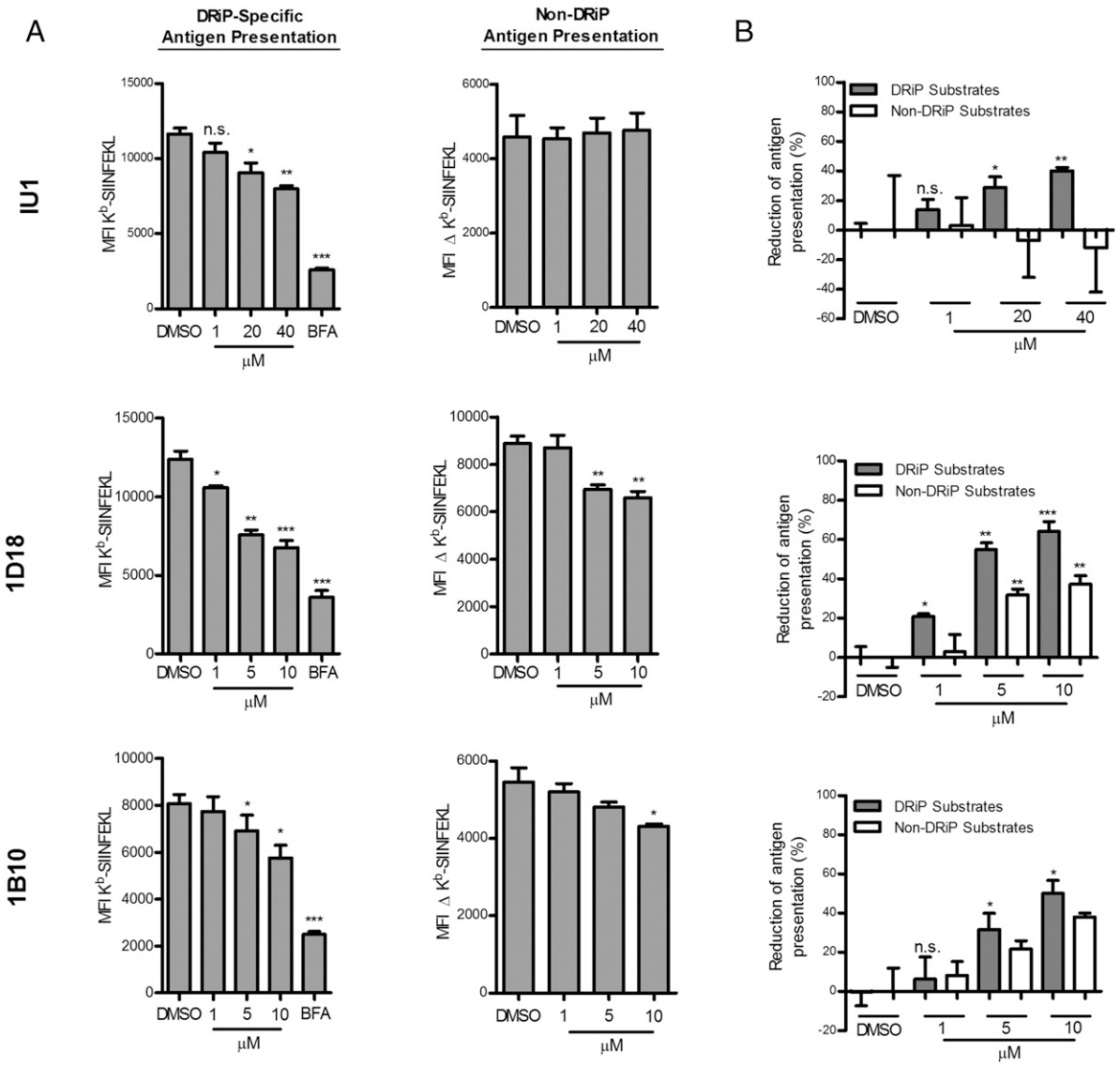

FIGURE 3. Chemical inhibition of Usp14 diminished DRiP K^b-SIINFEKL antigenic presentation. EL4/SCRAP-mCherry cells were used to monitor the effects of Ag presentation with Usp14 inhibition by IU1, 1D18, and 1B10. (**A**) Cells were acid washed to remove existing K^b-SIINFEKL complexes and cultured in the presence of Shield-1 or ethanol and various concentrations of IU1, 1D18, and 1B10. After 5 h of culture, cells were stained in triplicate with 25D-1.16 mAb. Ag presentation levels from non-DRiP substrates were determined by subtracting the MFI of 25D-1.16 staining of Shield-1–treated cells from the MFI of ethanol-treated cells. (**B**) Data from (A) are expressed as a percentage inhibition of Ag presentation. The range of K^b-SIINFEKL for non-DRiP substrates was determined by subtracting the MFI of 25D-1.16 staining of Shield-1–treated cells from ethanol-treated cells. For DRiP substrates (shaded bars) the range was determined by subtracting the MFI of 25D-1.16 staining of BFA-treated cells from Shield-1–treated cells. $*p < 0.05$, $**p < 0.01$, $***p < 0.001$. n.s., not significant.

SCRAP-mCherry following Shield-1 removal to be 41 ± 5 min. Treatment with the Usp14 inhibitors led to a slight increase in the half-life of SCRAP-mCherry protein, although the results were not statistically significant (ANOVA, $p > 0.05$). Conversely, inhibition of the proteasome with MG-132 not only prevented existing SCRAP-mCherry from being degraded but also rescued newly synthesized protein from degradation (Fig. 4A), resulting in an increased fluorescence signal. As previously stabilized SCRAP-mCherry is degraded following Shield-1 removal, there is a statistically significant increase in K^b-SIINFEKL complexes detected at the cell surface as depicted in Fig. 4B, where the number of precursor substrates degraded, as determined by mCherry fluorescence at time 0, yields an increase in peptide–MHC complexes at 2 h after Shield-1 removal. The difference in 25D-1.16 staining between Shield-1–treated cells and those treated with ethanol alone can be used to infer the presentation of peptides from retired substrates. Usp14 inhibition by 1D18 and 1B10 resulted in a slight decrease in retiree presentation whereas IU1 treatment did not diminish retiree presentation (Fig. 4C). Therefore, small molecule inhibition of Usp14 did not greatly alter the ability of the proteasome to degrade destabilized SCRAP-mCherry protein but did partially inhibit presentation of peptides from retired substrates.

To further examine the role of Usp14 in direct Ag presentation, we stably transfected DNA constructs encoding WT and catalytically inactive human Usp14-GFP into EL4/SCRAP-mCherry cells. Catalytically inactive Usp14 contains a point mutation that changes the active site cysteine to an alanine residue and the gene product acts as a DN form of Usp14 (16). We examined the effect of DN Usp14 in the presence of Shield-1 and compared it to transfected cells expressing the WT Usp14. We noted that cells expressed different levels of the SCRAP-mCherry protein (Fig. 5A) and therefore normalized K^b-SIINFEKL expression to mCherry

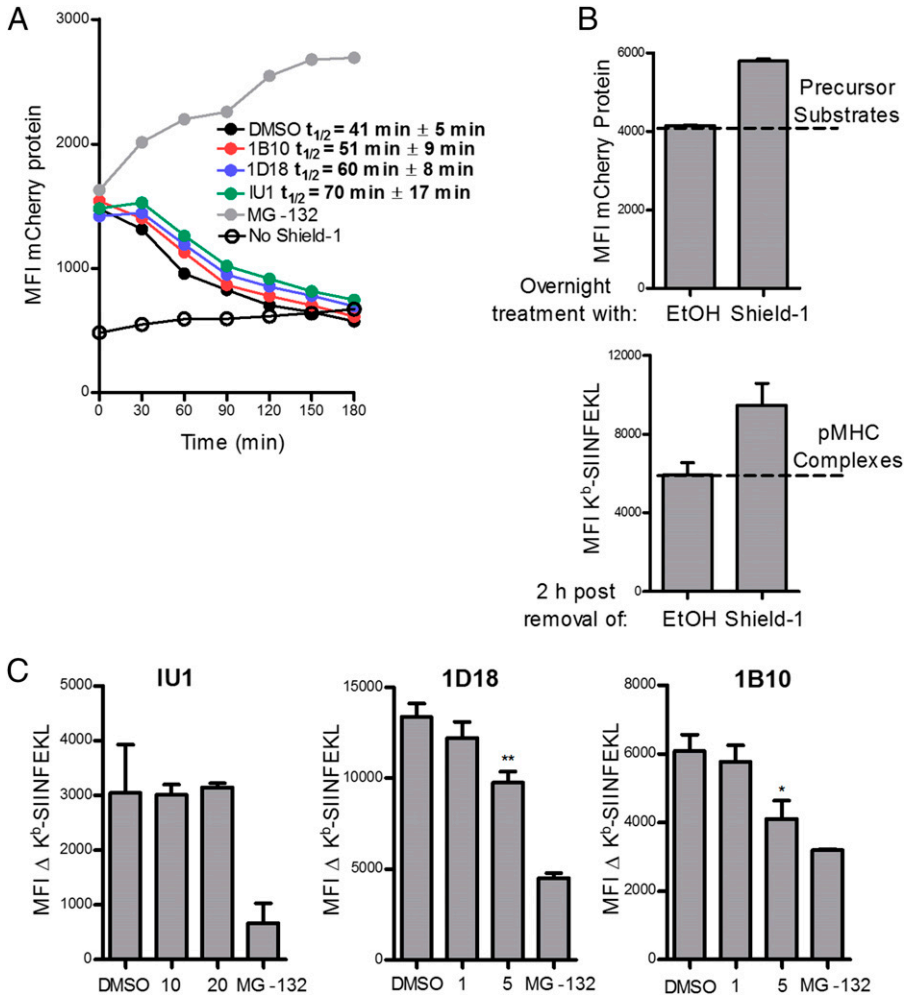

FIGURE 4. Chemical inhibition of Usp14 with 1D18 and 1B10 reduces retiree protein degradation. EL4/SCARP-mCherry cells were treated with Shield-1 for 18 h and then acid washed to remove K^b-SIINFEKL complexes and cultured without Shield-1 and in the presence of MG-132 (10 μM) or the Usp14 inhibitors IU1 (20 μM), 1D18 (5 μM), or 1B10 (5 μM) for 3 h (**A**) or 2 h (**B** and **C**). (A) SCRAP-mCherry protein degradation is shown at the indicated time points and the calculated half-life for the model protein in the presence of each inhibitor is listed. (B) Representative graphs demonstrating (top) the amount of precursor substrates from mCherry that contribute to (bottom) the number of K^b-SIINFEKL complexes observed in the retiree Ag presentation model. The difference in MFI of 25D-1.16 staining between cells with retired SCRAP-mCherry (labeled Shield-1) and cells treated with ethanol alone is termed the ΔK^b-SIINFEKL. (C) Usp14 inhibitors IU1, 1D18, and 1B10 at indicated concentrations were added to cells with retired SCRAP-mCherry and the ΔK^b-SIINFEKL was determined 2 h after Shield-1 removal. $*p < 0.05$, $**p < 0.01$.

levels to account for differences in peptide–MHC complexes due to the abundance of the precursor substrate. Expression of DN Usp14 did not alter the degradation rate of SCRAP-mCherry as compared with control cells expressing the WT Usp14 (Fig. 5A), and the half-life of SCRAP-mCherry in these cells is similar to the parental cell type (see Fig. 4A). Presentation of SIINFEKL peptides from retired SCRAP-mCherry was similar between cells expressing either WT or DN Usp14 (Fig. 5B). Similar to chemical inhibition of Usp14, expression of DN Usp14 resulted in a decrease in DRiP-specific Ag presentation (Fig. 5C). Because the levels of SCRAP-mCherry are different between cell types, it is necessary to normalize the levels of K^b-SIINFEKL to mCherry fluorescence to determine whether lower peptide–MHC levels are due to loss of Usp14 function or simply due to lower substrate levels. As shown in Fig. 5D, when K^b-SIINFEKL staining is normalized to mCherry signal, DRiP presentation is still reduced in cells expressing DN Usp14.

Despite its important role in trimming the polyubiquitin chains from substrates prior to proteasomal degradation, inhibition of Usp14 does not increase the levels of polyubiquitinated proteins in cells (19, 23). Our previous work has demonstrated that chemicals that specifically disrupt DRiP presentation can also increase levels of polyubiquitinated substrates in cells, suggesting a link between polyubiquitin chain disassembly and Ag presentation (13). To determine whether Usp14 disruption increased polyubiquitinated proteins in our cells, we analyzed whole-cell lysates by Western blot for polyubiquitinated proteins. Cells were treated with IU1, 1D18, 1B10, or MG-132 for 3 h and lysed by boiling SDS-PAGE buffer, which solubilizes nearly all proteins within the cell. Western blot analysis revealed that Usp14-inhibiting compounds did not increase levels of polyubiquitinated proteins within the cell when used at concentrations that inhibit direct Ag presentation (Fig. 6A). Additionally, expression of DN Usp14 did not increase levels of polyubiquitinated substrates compared with cells expressing WT Usp14 (Fig. 6B). These results confirm that Usp14 inhibition does not increase levels of polyubiquitinated proteins within cells in the same manner as proteasome inhibition.

Finally, we tested the effect of Usp14 chemical inhibitors on cells expressing DN Usp14. Although compounds 1D18 and 1B10 inhibited DRiP Ag presentation in cells expressing WT Usp14, neither drug statistically reduced DRiP Ag presentation in cells expressing DN Usp14 (Fig. 7). These data demonstrate that these agents do in fact target Usp14 in cells and that genetic inhibition of DRiP presentation cannot be further enhanced by treatment with the small-molecule inhibitors.

Discussion

A functional proteasome is necessary for the degradation of many, although not all, proteins that contain antigenic peptides destined for presentation on MHC class I molecules. It is therefore necessary to understand how different subunits of the proteasome function to manipulate direct Ag presentation. In this study we examined the role of a specific proteasome-associated DUB, Usp14, and found that chemical inhibition of Usp14 and expression of catalytically inactive forms of the protein negatively impact direct Ag presentation, which is particularly true for DRiP forms of the model

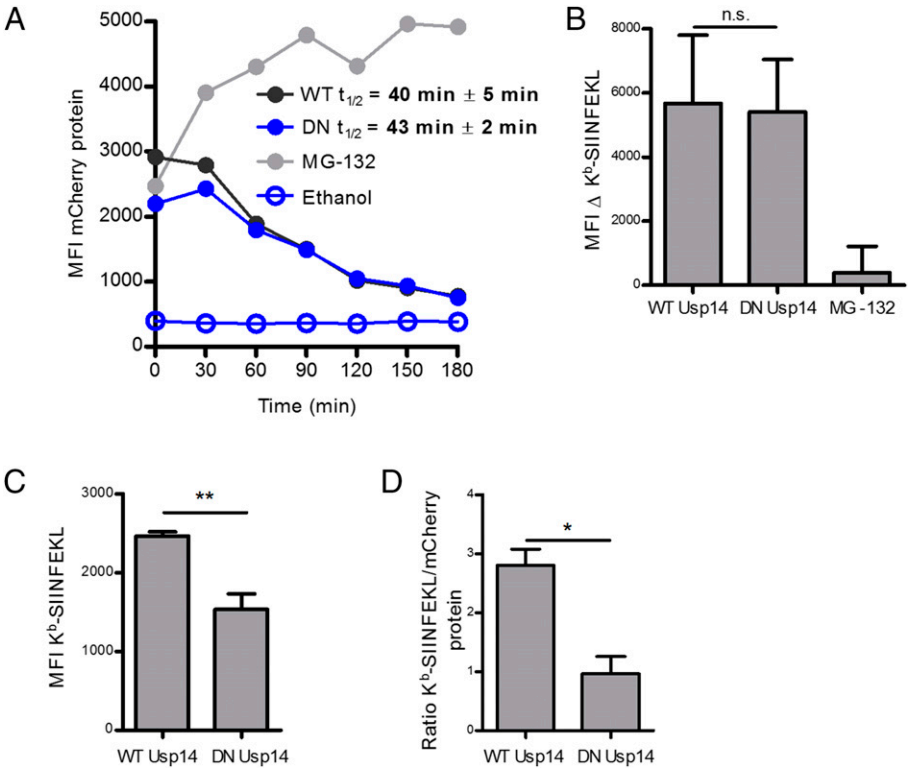

FIGURE 5. Catalytically inactive DN Usp14 diminishes DRiP K^b-SIINFEKL presentation. (**A**) Catalytically deficient DN Usp14 was used to measure effects of Usp14 on Ag presentation. (A) Shield-1 treatment (1 μM) of EL4 SCRAP-mCherry cells expressing WT or DN Usp14 for 18 h and subsequent Shield-1 removal allowed the determination of mCherry protein half-life. (**B**) K^b-SIINFEKL differences between Shield-1 and ethanol treatment were measured in either Usp14 WT or DN cells 2 h following the removal of Shield-1 and compared with MG-132–treated cells. (**C**) Usp14 WT and Usp14 DN cells were first washed with mild acidic buffer and then treated with Shield-1 or ethanol and monitored for K^b-SIINFEKL presentation after 5 h. Cells were stained in triplicate to determine K^b-SIINFEKL levels. (**D**) To account for differences in mCherry levels between the cell types, the MFI of K^b-SIINFEKL signal was normalized to mCherry protein accumulation. $*p < 0.05$, $**p < 0.05$. n.s., not significant.

protein when compared with retired SCRAP-mCherry. This corroborates the work of Fiebiger et al. (22) who found that broadly inhibiting proteasomal DUBs prevented direct Ag presentation, although this stands in contrast to Qian et al. (24) who found that the presentation of vaccinia virus–derived DRiPs occurred independently of the DUB activity of the 19S subunit. Although there are many differences between the experimental setups, both our data and the data of Fiebiger et al. (15) were obtained from model Ags expressed as self-genes via transfection, whereas Qian et al. (24) measured direct presentation from viral genes, suggesting that perhaps the source of the antigenic peptide may dictate the necessity for proteasome deubiquitination. We have previously demonstrated that the efficiency of Ag presentation is different when a protein is expressed from a transfected plasmid compared with a virally expressed gene product (15), demonstrating that viral and self-antigens may be differentially recognized by the cell.

Inhibition of Usp14 is recognized to accelerate the degradation of substrates by the proteasome (19). Indeed, both chemical and genetic inhibition of Usp14 can help cells eliminate misfolded proteins, including clinically relevant proteins such as PrP, Tau, Htt, and TDP-43, which have been implicated in different neurologic disorders (19, 25, 26). It would therefore seem contradictory that Usp14 inhibition would reduce presentation of peptides, especially from DRiPs that can be misfolded proteins (27) whose degradation should be accelerated when Usp14 is inhibited. Usp14 is also necessary for interacting with ubiquitin moieties and proteasome gate opening (28), allowing substrates to access the catalytic core of the proteasome. When compared with proteasome inhibition (Fig. 4A), Usp14 inhibition with both

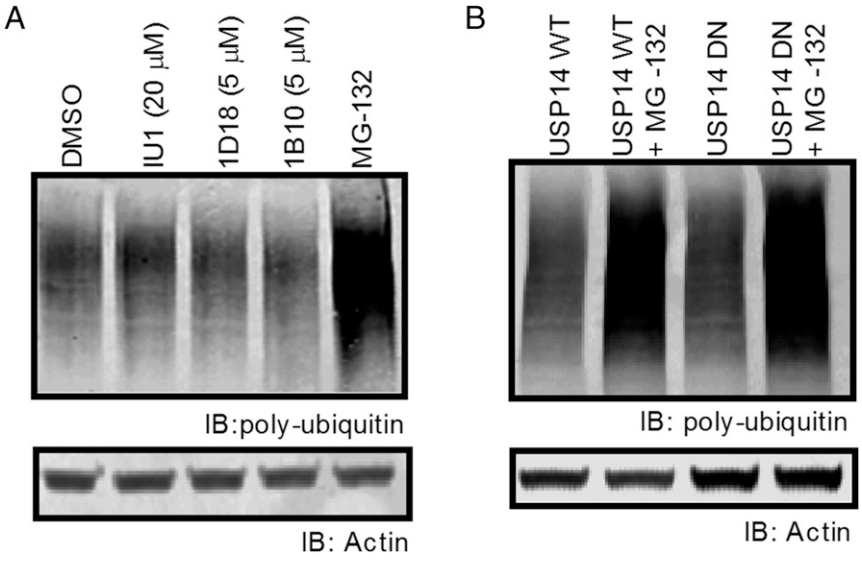

FIGURE 6. Polyubiquitinated protein levels are not changed upon Usp14 inhibition. Polyubiquitinated protein levels of cells treated with either IU1, 1D18, 1B10, or cells containing the DN phenotype for Usp14 were measured by Western blot. (**A**) Polyubiquitin staining with FK2 monoclonal mouse Ab after 2 h treatment with vehicle, IU1 (20 μM), 1D18 (5 μM), 1B10 (5 μM), or 10 μM MG-132. (**B**) Cell lysates from WT Usp14 and DN Usp14 were untreated or incubated with MG-132 for 2 h and then stained for polyubiquitin. Actin Ab was used as a loading control for all polyubiquitin Western blots.

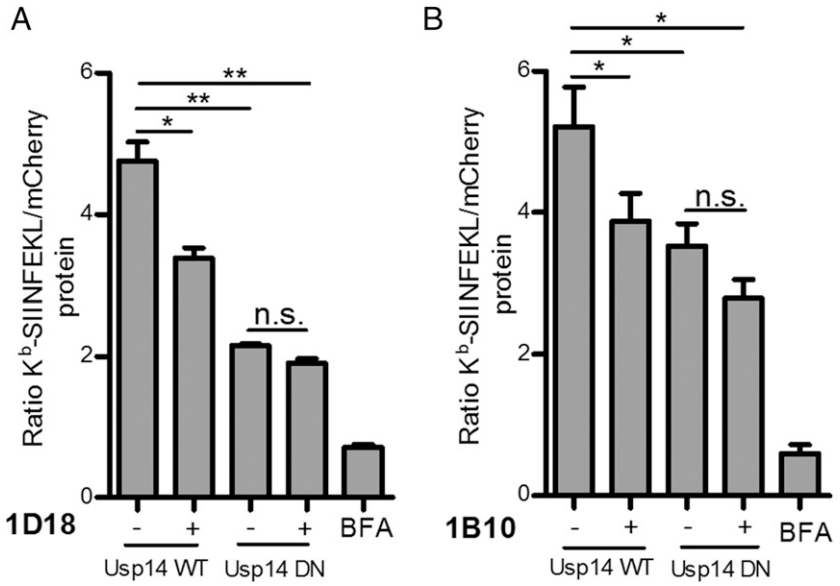

FIGURE 7. Chemical inhibition of Usp14 in cells containing catalytically inactive Usp14 does not further diminish antigenic peptide presentation. Effects of both Usp14 inhibition, with chemical compounds, and the DN form of Usp14 on DRiP Ag presentation was measured. WT Usp14 WT and DN Usp14 cells treated with 5 μM of 1B10 (**A**) or 1D18 (**B**) for 5 h and aliquots of cell suspension were analyzed by flow cytometry for the detection of K^b-SIINFEKL complexes and mCherry fluorescence. K^b-SIINFEKL was normalized to mCherry protein accumulation. BFA was added to a portion of cells to act as a positive control for complete reduction of Ag presentation. *$p < 0.05$, **$p < 0.01$. n.s., not significant.

chemical inhibitors and by expression of catalytically inactive Usp14 did not appreciably reduce the rate at which previously stabilized SCRAP-mCherry was degraded upon Shield-1 removal, although a modest increase in substrate half-life was observed upon chemical inhibition. These data suggest that proteasome function was not compromised in the conditions of our experiments. However, the effect of altered proteasome function may be more pronounced on peptide production than SCRAP-mCherry degradation. This may explain why direct Ag presentation was reduced when Usp14 was inhibited. Usp14 has also recently been shown to specifically recognize a substrate with multiple ubiquitin chains, suggesting that Usp14 has substrate specificity (29). We and others have suggested that DRiP Ag presentation may occur via different molecular mechanisms than presentation of peptides from retired proteins (13, 30, 31) and may in fact be compartmentalized (14). Perhaps DRiPs are marked in a particular manner to interact with Usp14 facilitating their degradation and efficient presentation.

Given that Usp14 can interact with and process ubiquitinated substrates, it is somewhat surprising that expression of DN forms of ubiquitin within cells, in many instances, does not eliminate Ag presentation (32). Additionally, mutation of antigenic substrates to remove amino acids capable of being the target of ubiquitination (notably lysine, but also cysteine, seine, and threonine) does not eliminate the ability of a substrate to be degraded and for peptides to be presented (22). Furthermore, the effect of ubiquitin conjugation inhibitors on Ag presentation can vary based upon many factors, including the source of the peptide and the particular MHC class I allele studied (33). Therefore, it may not be necessary for a substrate to be ubiquitinated to be degraded and presented. These findings complicate our interpretation of the role of Usp14 in direct Ag presentation. However, Usp14 is also known to inhibit the unfolded protein response (UPR) through its interactions with IRE1α (26, 34, 35). Inhibition or depletion of Usp14 is known to increase the UPR, which can inhibit ongoing protein synthesis, a process necessary for the creation of DRiPs. Indeed, activating the UPR is known to decrease Ag presentation, especially of cytosolic Ags (36). It is therefore possible that the inhibition of Usp14 is due to induction of the UPR and may not involve the ubiquitin–proteasome system. In either case the mystery of substrate ubiquitination, proteasomal deubiquitination, and Ag presentation is far from solved and undoubtedly more complex than suspected.

Disclosures

The authors have no financial conflicts of interest.

References

1. van Endert, P. 2011. Post-proteasomal and proteasome-independent generation of MHC class I ligands. *Cell. Mol. Life Sci.* 68: 1553–1567.
2. Lee, M. J., B.-H. Lee, J. Hanna, R. W. King, and D. Finley. 2011. Trimming of ubiquitin chains by proteasome-associated deubiquitinating enzymes. *Mol. Cell. Proteomics* 10: R110.003871.
3. Kim, H. M., Y. Yu, and Y. Cheng. 2011. Structure characterization of the 26S proteasome. *Biochim. Biophys. Acta.* 1809: 67–79.
4. Setz, C., M. Friedrich, S. Hahn, J. Dörrie, N. Schaft, G. Schuler, and U. Schubert. 2013. Just one position-independent lysine residue can direct MelanA into proteasomal degradation following N-terminal fusion of ubiquitin. *PLoS One* 8: e55567.
5. Rodriguez, F., J. Zhang, and J. L. Whitton. 1997. DNA immunization: ubiquitination of a viral protein enhances cytotoxic T-lymphocyte induction and antiviral protection but abrogates antibody induction. *J. Virol.* 71: 8497–8503.
6. Antón, L. C., and J. W. Yewdell. 2014. Translating DRiPs: MHC class I immunosurveillance of pathogens and tumors. *J. Leukoc. Biol.* 95: 551–562.
7. Dolan, B. P., J. R. Bennink, and J. W. Yewdell. 2011. Translating DRiPs: progress in understanding viral and cellular sources of MHC class I peptide ligands. *Cell. Mol. Life Sci.* 68: 1481–1489.
8. Princiotta, M. F., D. Finzi, S. B. Qian, J. Gibbs, S. Schuchmann, F. Buttgereit, J. R. Bennink, and J. W. Yewdell. 2003. Quantitating protein synthesis, degradation, and endogenous antigen processing. *Immunity* 18: 343–354.
9. Qian, S. B., E. Reits, J. Neefjes, J. M. Deslich, J. R. Bennink, and J. W. Yewdell. 2006. Tight linkage between translation and MHC class I peptide ligand generation implies specialized antigen processing for defective ribosomal products. *J. Immunol.* 177: 227–233.
10. Bourdetsky, D., C. E. H. Schmelzer, and A. Admon. 2014. The nature and extent of contributions by defective ribosome products to the HLA peptidome. *Proc. Natl. Acad. Sci. USA* 111: E1591–E1599.
11. Croft, N. P., S. A. Smith, Y. C. Wong, C. T. Tan, N. L. Dudek, I. E. Flesch, L. C. Lin, D. C. Tscharke, and A. W. Purcell. 2013. Kinetics of antigen expression and epitope presentation during virus infection. *PLoS Pathog.* 9: e1003129.
12. Porgador, A., J. W. Yewdell, Y. Deng, J. R. Bennink, and R. N. Germain. 1997. Localization, quantitation, and in situ detection of specific peptide–MHC class I complexes using a monoclonal antibody. *Immunity* 6: 715–726.
13. Dolan, B. P., L. Li, C. A. Veltri, C. M. Ireland, J. R. Bennink, and J. W. Yewdell. 2011. Distinct pathways generate peptides from defective ribosomal products for CD8$^+$ T cell immunosurveillance. *J. Immunol.* 186: 2065–2072.
14. Lev, A., M. F. Princiotta, D. Zanker, K. Takeda, J. S. Gibbs, C. Kumagai, E. Waffarn, B. P. Dolan, A. Burgevin, P. Van Endert, et al. 2010. Compartmentalized MHC class I antigen processing enhances immunosurveillance by circumventing the law of mass action. *Proc. Natl. Acad. Sci. USA* 107: 6964–6969.
15. Dolan, B. P., A. A. Sharma, J. S. Gibbs, T. J. Cunningham, J. R. Bennink, and J. W. Yewdell. 2012. MHC class I antigen processing distinguishes endogenous antigens based on their translation from cellular vs. viral mRNA. *Proc. Natl. Acad. Sci. USA* 109: 7025–7030.
16. de Jong, A., R. Merkx, I. Berlin, B. Rodenko, R. H. Wijdeven, D. El Atmioui, Z. Yalçin, C. N. Robson, J. J. Neefjes, and H. Ovaa. 2012. Ubiquitin-based probes prepared by total synthesis to profile the activity of deubiquitinating enzymes. *ChemBioChem* 13: 2251–2258.

17. Palmer, A. L., and B. P. Dolan. 2013. MHC class I antigen presentation of DRiP-derived peptides from a model antigen is not dependent on the AAA ATPase p97. *PLoS One* 8: e67796.
18. Ekkebus, R., S. I. van Kasteren, Y. Kulathu, A. Scholten, I. Berlin, P. P. Geurink, A. de Jong, S. Goerdayal, J. Neefjes, A. J. Heck, et al. 2013. On terminal alkynes that can react with active-site cysteine nucleophiles in proteases. *J. Am. Chem. Soc.* 135: 2867–2870.
19. Lee, B.-H., M. J. Lee, S. Park, D.-C. Oh, S. Elsasser, P.-C. Chen, C. Gartner, N. Dimova, J. Hanna, S. P. Gygi, et al. 2010. Enhancement of proteasome activity by a small-molecule inhibitor of USP14. *Nature* 467: 179–184.
20. Banaszynski, L. A., L. C. Chen, L. A. Maynard-Smith, A. G. Ooi, and T. J. Wandless. 2006. A rapid, reversible, and tunable method to regulate protein function in living cells using synthetic small molecules. *Cell* 126: 995–1004.
21. Cram, E. D., R. S. Simmons, A. L. Palmer, W. H. Hildebrand, D. D. Rockey, and B. P. Dolan. 2015. Enhanced direct major histocompatibility complex class I self-antigen presentation induced by *Chlamydia* infection. *Infect. Immun.* 84: 480–490.
22. Fiebiger, B. M., A. Moosmann, U. Behrends, and J. Mautner. 2012. Mature proteins derived from Epstein-Barr virus fail to feed into the MHC class I antigenic pool. *Eur. J. Immunol.* 42: 3167–3173.
23. Chen, P.-C., L.-N. Qin, X.-M. Li, B. J. Walters, J. A. Wilson, L. Mei, and S. M. Wilson. 2009. The proteasome-associated deubiquitinating enzyme Usp14 is essential for the maintenance of synaptic ubiquitin levels and the development of neuromuscular junctions. *J. Neurosci.* 29: 10909–10919.
24. Qian, S. B., M. F. Princiotta, J. R. Bennink, and J. W. Yewdell. 2006. Characterization of rapidly degraded polypeptides in mammalian cells reveals a novel layer of nascent protein quality control. *J. Biol. Chem.* 281: 392–400.
25. Homma, T., D. Ishibashi, T. Nakagaki, T. Fuse, T. Mori, K. Satoh, R. Atarashi, and N. Nishida. 2015. Ubiquitin-specific protease 14 modulates degradation of cellular prion protein. *Sci. Rep.* 5: 11028.
26. Hyrskyluoto, A., C. Bruelle, S. H. Lundh, H. T. Do, J. Kivinen, E. Rappou, S. Reijonen, T. Waltimo, Å. Petersén, D. Lindholm, and L. Korhonen. 2014. Ubiquitin-specific protease-14 reduces cellular aggregates and protects against mutant huntingtin-induced cell degeneration: involvement of the proteasome and ER stress-activated kinase IRE1α. *Hum. Mol. Genet.* 23: 5928–5939.
27. Anton, L. C., J. W. Yewdell, and J. R. Bennink. 1997. MHC class I-associated peptides produced from endogenous gene products with vastly different efficiencies. *J. Immunol.* 158: 2535–2542.
28. Peth, A., H. C. Besche, and A. L. Goldberg. 2009. Ubiquitinated proteins activate the proteasome by binding to Usp14/Ubp6, which causes 20S gate opening. *Mol. Cell* 36: 794–804.
29. Lee, B.-H., Y. Lu, M. A. Prado, Y. Shi, G. Tian, S. Sun, S. Elsasser, S. P. Gygi, R. W. King, and D. Finley. 2016. USP14 deubiquitinates proteasome-bound substrates that are ubiquitinated at multiple sites. *Nature* 532: 398–401.
30. Apcher, S., C. Daskalogianni, F. Lejeune, B. Manoury, G. Imhoos, L. Heslop, and R. Fåhraeus. 2011. Major source of antigenic peptides for the MHC class I pathway is produced during the pioneer round of mRNA translation. *Proc. Natl. Acad. Sci. USA* 108: 11572–11577.
31. Apcher, S., G. Millot, C. Daskalogianni, A. Scherl, B. Manoury, and R. Fåhraeus. 2013. Translation of pre-spliced RNAs in the nuclear compartment generates peptides for the MHC class I pathway. *Proc. Natl. Acad. Sci. USA* 110: 17951–17956.
32. Huang, L., J. M. Marvin, N. Tatsis, and L. C. Eisenlohr. 2011. Cutting edge: selective role of ubiquitin in MHC class I antigen presentation. *J. Immunol.* 186: 1904–1908.
33. Wei, J., D. Zanker, A. R. Di Carluccio, M. G. Smelkinson, K. Takeda, M. O. Seedhom, D. Dersh, J. S. Gibbs, N. Yang, A. Jadhav, et al. 2017. Varied role of ubiquitylation in generating MHC class I peptide ligands. *J. Immunol.* 198: 3835–3845.
34. Nagai, A., H. Kadowaki, T. Maruyama, K. Takeda, H. Nishitoh, and H. Ichijo. 2009. USP14 inhibits ER-associated degradation via interaction with IRE1α. *Biochem. Biophys. Res. Commun.* 379: 995–1000.
35. Perry, J. W., M. Ahmed, K.-O. Chang, N. J. Donato, H. D. Showalter, and C. E. Wobus. 2012. Antiviral activity of a small molecule deubiquitinase inhibitor occurs via induction of the unfolded protein response. *PLoS Pathog.* 8: e1002783.
36. Granados, D. P., P.-L. Tanguay, M.-P. Hardy, E. Caron, D. de Verteuil, S. Meloche, and C. Perreault. 2009. ER stress affects processing of MHC class I-associated peptides. *BMC Immunol.* 10: 10.